Journal of Cell Science 108, 3145-3154 (1995)
Printed in Great Britain © The Company of Biologists Limited 1995

The membrane skeleton of acetylcholine receptor domains in rat myotubes contains antiparallel homodimers of β-spectrin in filaments quantitatively resembling those of erythrocytes

David W. Pumplin

Department of Anatomy, University of Maryland at Baltimore, 655 W. Baltimore Street, Baltimore, MD 21201, USA

e-mail: dpumplin@umabnet.ab.umd.edu

SUMMARY

I used immunogold labeling and quick-freeze, deep-etch, rotary replication to characterize the membrane skeleton at regions with high concentrations of acetylcholine receptor domains in receptor clusters of cultured rat muscle cells. This membrane skeleton consists of a network of filaments closely applied to the cytoplasmic membrane surface. The filaments are specifically decorated by immunogold labeling with a monoclonal antibody, VIIF7, that recognizes an isoform of β-spectrin colocalizing with acetylcholine receptors. The filaments are 32±11 nm in length and three to four filaments (average 3.1-3.3) join at each intersection to form the network. These parameters are nearly identical to those reported previously for the membrane skeleton of erythrocytes. Depending on the amount of platinum coating, filament diameters range from 9 to 11 nm in diameter, and are 1.4 nm larger on average than spectrin filaments of erythrocytes replicated at the same time. Filaments are decorated with gold particles close to one end, consistent with the location of the epitope recognized by the monoclonal antibody. Computer modeling shows that all filament intersections in the membrane skeletal network are equally capable of being labeled by the monoclonal antibody. This pattern of labeling is consistent with a network containing antiparallel homodimers of β-spectrin.

Key words: spectrin, acetylcholine receptor, cytoskeleton, muscle cell

INTRODUCTION

Acetylcholine receptors (AChRs) become concentrated in the postsynaptic membrane early in the development of the neuromuscular junction. To understand how this occurs, numerous efforts have aimed at identifying proteins of the postsynaptic cytoskeleton and studying their relationship to AChR by biochemical and immunological techniques (reviewed by Bloch and Pumplin, 1988; Froehner, 1993). Concurrently, the organization of AChR and the cytoskeleton of the postjunctional membrane have been investigated with ultrastructural techniques (Birks et al., 1960; Tatsuoka et al., 1988). Although rapid freezing and etching revealed a network of filaments attached to the inner surface of the postsynaptic membrane (Hirokawa and Heuser, 1982), proteins contained in this network were not identified.

In order to understand how particular proteins contribute to the structure of the postsynaptic membrane, I studied the clusters of AChR that form in ventral membranes of cultured myotubes. These offer a useful model for the postsynaptic apparatus of embryonic neuromuscular junctions (reviewed by Bloch and Pumplin, 1988). AChR clusters in substrate-attached ventral membranes of muscle cells are isolated by extracting other portions of the cells with mild detergent or mechanical shearing with a stream of buffer. Cytoplasmic surfaces of the membranes are readily accessible for ultrastructural examination by quick-freeze, deep-etch, rotary replication (QFDERR; Pumplin, 1989) and protein localization by immunolabeling (Bloch et al., 1991; Dmytrenko et al., 1993). AChR-rich domains contain a high concentration of receptors (1,000-2,000/μm^2; see references in Bloch and Pumplin, 1988) that are nearly immobile (Axelrod et al., 1978; Stya and Axelrod, 1983). Corresponding intramembrane particles are uniformly distributed, and this even distribution is dependent on metabolic energy (Pumplin and Bloch, 1987). QFDERR of clusters reveals a membrane skeleton consisting of a network of short filaments closely applied to the inner surface of the membrane at AChR domains (Pumplin, 1989). Taken together, these findings suggest that many AChR molecules are anchored in some fashion to this network.

Immunofluorescence studies show that the membrane skeleton of AChR clusters contains an unusual isoform of β-spectrin (Bloch and Morrow, 1989; Daniels, 1990) as well as the 43 kDa receptor-associated protein (Bloch and Froehner, 1987; Froehner, 1993) and a 58 kDa protein (Bloch et al., 1991) now termed syntrophin. Semiquantitative fluorescence measurements demonstrate that these proteins are present in a ratio of 1 43 kDa, 1 syntrophin, and 4-7 β-spectrin molecules per molecule of AChR. Clusters also contain smaller but significant amounts of dystrophin (Dmytrenko et al, 1993) and

utrophin (R. J. Bloch et al., unpublished observations). Brief treatment of clusters with chymotrypsin removes β-spectrin and other membrane skeletal proteins and allows AChR to disperse, suggesting that these proteins are important in maintaining the organization of AChR (Bloch and Morrow, 1989; Bloch et al., 1991; Dmytrenko et al., 1993). Actin is also present in AChR domains and is removed together with spectrin by treatment with low ionic strength solutions or chymotrypsin, but the molar ratio between these proteins was not determined (Bloch, 1986). Based on these data and the well-studied membrane skeleton of erythrocytes (Marchesi, 1985; Bennett, 1990), Bloch and Morrow (1989) proposed a model for the membrane skeleton of AChR domains containing dimers of spectrin linked head-to-head and binding via their tails to oligomers of actin. Unlike the erythrocyte, the membrane skeleton at AChR domains was postulated to contain only β-spectrin subunits, as no α-spectrin subunit could be identified. To test this model experimentally, I compared the membrane skeletons of AChR domains with those of erythrocytes, using quantitative analyses of ultrastructure and immunolocalization. The membrane skeletons of erythrocytes and AChR domains contain filaments of nearly identical size and connectivity. The pattern of immunogold labeling is consistent with a network of filaments composed of antiparallel homodimers of β-spectrin.

MATERIALS AND METHODS

Myotube culture and isolation of AChR clusters

Muscle cells were isolated from hind limbs of neonatal rats, as described previously (Bloch, 1979; Bloch and Geiger, 1980), and cultured on glass coverslips in Dulbecco-Vogt modified Eagle's medium (DMEM; Gibco, Grand Island, NY) supplemented with 10% fetal calf serum. Cultures 6-8 days old were stained for 30 minutes at room temperature (RT) with tetramethylrhodamine-α-bungarotoxin (R-BT), prepared as previously reported (Ravdin and Axelrod, 1977) and diluted to a final concentration of 5 μg/ml in HEPES-buffered DMEM supplemented with 5% fetal calf serum.

For isolation of clusters, myotubes stained with R-BT were treated for 2 minutes with a solution containing zinc (1 mM $ZnCl_2$, 3 mM EGTA, 5 mM $MgCl_2$, 100 mM PIPES, pH 6.0; Avnur and Geiger, 1981), then sheared with a stream of buffer containing a high concentration of K^+ (100 mM KCl, 5 mM $MgCl_2$, 3 mM EGTA, 20 mM HEPES, pH 7.0; Aggeler and Werb, 1982) and immediately fixed in cold 2% paraformaldehyde in the same buffer.

Ultrastructural methods

Immunogold labeling and QFDERR of clusters were performed with the methods and precautions described previously (Pumplin et al., 1990; Dmytrenko et al., 1993). In brief, clusters were isolated by shearing, fixed in paraformaldehyde, and labeled for 1 hour at RT with anti-β-spectrin mAb VIIF7 (Harris et al., 1986) diluted 1:50, followed by fluoresceinated rabbit anti-mouse IgG (1:100 in 1% bovine serum albumin (BSA) in phosphate-buffered saline (PBS), 1 hour, RT). After washing, the samples were incubated overnight at 4°C with goat anti-rabbit IgG adsorbed to 10 nm colloidal gold (Janssen Pharmaceuticals, Beerse, Belgium), diluted 1:10 in BANT (0.1% BSA, 0.5 M NaCl, 10 mM $MgCl_2$, 20 mM Tris-HCl, 20 mM NaN_3, pH 7.4; Luther and Bloch, 1989). Well-formed clusters were chosen by tetramethylrhodamine and fluorescein fluorescence, photographed, and their positions circled with a diamond marking objective. Concentric circles (4 mm diameter) were scribed around these identified clusters and then broken out of the coverslips. Samples were further fixed in 2% glutaraldehyde, then rinsed 3 times in PBS followed by a rinse in D_2O. After removal of nearly all the overlying liquid, the samples were rapidly frozen by being pressed against a metal mirror at −196°C. Frozen samples were freeze-dried at −95°C under high vacuum until D_2O sublimation ceased, then rotary replicated with platinum applied at an angle of 20°, followed by a backing layer of carbon. Replicated clusters were readily relocated by reference to the previously scribed circle. They were floated off the coverslips in 5% HF, rinsed in water, and picked up on Formvar-coated slot grids. Electron micrographs were taken at low magnification (×1,400) to compare with corresponding fluorescence images and at high magnification (×44,000) in stereo pairs with ±6° of tilt.

Quantification of micrographs

Fluorescence and electron micrographs were digitized at high resolution by photographing them with a cooled, slow-scan CCD camera (Photometrics, Tucson, AZ). Filament diameters were measured with NIH Image software from digitized electron microscope negatives. Net magnification on the computer monitor was 6.3×10^5, and the smallest measurable distance was 0.6 nm. For analysis of filament lengths and immunogold labeling, one print of a stereo pair was digitized with the CCD camera and its filaments or intersections were traced with Aldus Freehand 3.1 (Altsys Corp., Seattle,WA). Tracings were printed onto transparency sheets, then overlain onto the original print to check for accuracy. From these tracings, the number of filaments at each intersection was counted, and filament lengths were measured with a graphics tablet and Bioquant software (RMS, Memphis, TN).

Statisical tests were performed and graphs drawn with Statview software (Abacus Concepts, Berkeley, CA).

RESULTS

AChR clusters in cultured rat myotubes were located by fluorescence of tetramethylrhodamine-α-bungarotoxin (R-BT), then isolated by mechanical shearing. Shearing cultured myotubes with a stream of buffer removed most of each cell, but portions of ventral membranes, together with particular cytoskeletal proteins that were firmly attached to these membranes, remained on the supporting coverslip and were examined by QFDERR. AChR domains in the resulting replicas were relocated by mapping to corresponding bright areas in fluorescence micrographs as described (Pumplin et al., 1990). Cytoskeletal proteins at AChR domains formed a membrane skeleton consisting of a distinctive network of filaments that were closely applied to the cytoplasmic surface of the membrane. Mapping fluorescence micrographs to replicas of the same cluster showed that boundaries of the network corresponded to the boundaries of fluorescence due to R-BT (Fig. 1). Thus, the network of filaments, or membrane skeleton, was present only in regions of membrane that were also highly enriched in AChR.

The network at AChR domains was composed of straight filaments intersecting with each other, and could be completely described by only three parameters: the lengths and diameters of the component filaments, and the average number of filaments at each intersection. These parameters were measured from micrographs of AChR domains that were not immunogold labeled, but were identified by mapping to locations of R-BT fluorescence and selected for a well-defined membrane skeleton that was not overlain by other cytoskeletal filaments (an example is shown in Fig. 2). Filament lengths

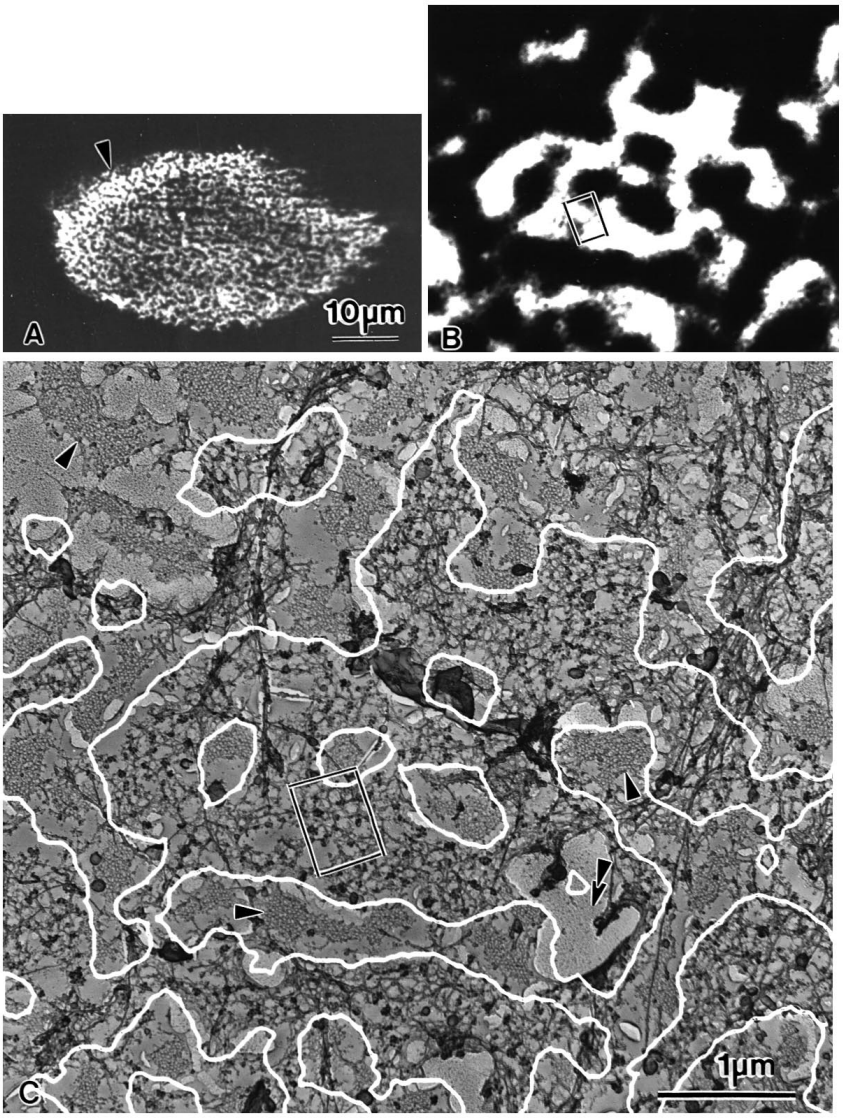

Fig. 1. A membrane skeleton colocalizes with membrane areas containing acetylcholine receptors. (A) Fluorescence micrograph of a cluster labeled with tetramethylrhodamine-α-bungarotoxin. The region indicated by the arrowhead in this micrograph is shown enlarged in a digitized image (B). Boundaries between areas rich and poor in fluorescence in B were determined by thresholding and edge tracing algorithms in the NIH Image program. These boundaries are shown as white lines superimposed on the electron micrograph of the same region after shearing and quick-freeze, deep-etch, rotary replication (C). Areas high in fluorescence have a distinctive membrane skeletal network, while membrane areas lacking fluorescence lie outside the cluster or correspond to plaques of clathrin (arrowheads). Occasionally, the membrane skeleton at a fluorescent area was torn away prior to replication (double arrowhead). One area that is rich in AChR and contains a well-defined network of filaments is indicated by boxes in B and C and shown at higher magnification in Fig. 5.

had a nearly Gaussian distribution (Fig. 3A) and were 32±11 nm in length (357 filaments; 4 micrographs; 3 clusters). Only a few filaments were as long as 70 nm. Repeated measurements of the same filament agreed within <1 nm, so the distribution histogram reflects real differences in filament lengths rather than measurement errors. Diameters of filaments in the same micrographs were also distributed normally (Fig. 3B), and were 8.6±2.0 nm in diameter (250 filaments; 4 micrographs from 3 clusters) including their platinum coat.

The mean diameter of filaments varied in different replicas. In order to compare directly the diameters of filaments in AChR clusters with those in erythrocytes, I replicated four identified clusters and two erythrocyte samples simultaneously, using the six-place sample holder described previously (Pumplin et al., 1990). Differences in the average diameters of filaments in AChR domains were highly correlated ($P<.0001$) with differences in the average diameters of filaments in networks of polymerized clathrin located ≤2 μm from these domains (Fig. 4), suggesting that both are due to variations in amount of deposited platinum. Nonetheless, filaments in AChR domains were somewhat larger (10.5±1.8 nm; 330 filaments; 6 clusters; 4 replicas) than those of erythrocytes (9.1±1.2 nm; 350 filaments; 7 cells; 2 replicas), suggesting that some additional proteins, as yet unidentified, must be present in filaments of AChR domains that are not found in erythrocytes.

Three to five filaments participated in each intersection. The average number of filaments/intersection (connectivity) was 3.1-3.3, quantified in the AChR domain shown in Fig. 2 and in two additional immunolabeled domains. The values of spectrin filament length, diameter, and connectivity were close to those previously measured for the spectrin-based membrane skeleton of erythrocyte ghosts viewed by QFDERR (Table 1).

In order to ascertain how β-spectrin contributes to the membrane skeleton of AChR domains, clusters isolated by shearing were labeled with mAb VIIF7 followed by a fluorescent secondary antibody and a tertiary antibody adsorbed to colloidal gold. Well-formed clusters were selected by fluorescence microscopy, photographed, and subjected to QFDERR. Fluorescence images (not shown) confirmed that β-spectrin labeling by mAb VIIF7 colocalized with AChR domains labeled by R-BT. Gold particles marking VIIF7 binding were also confined to AChR domains (Fig. 5A), iden-

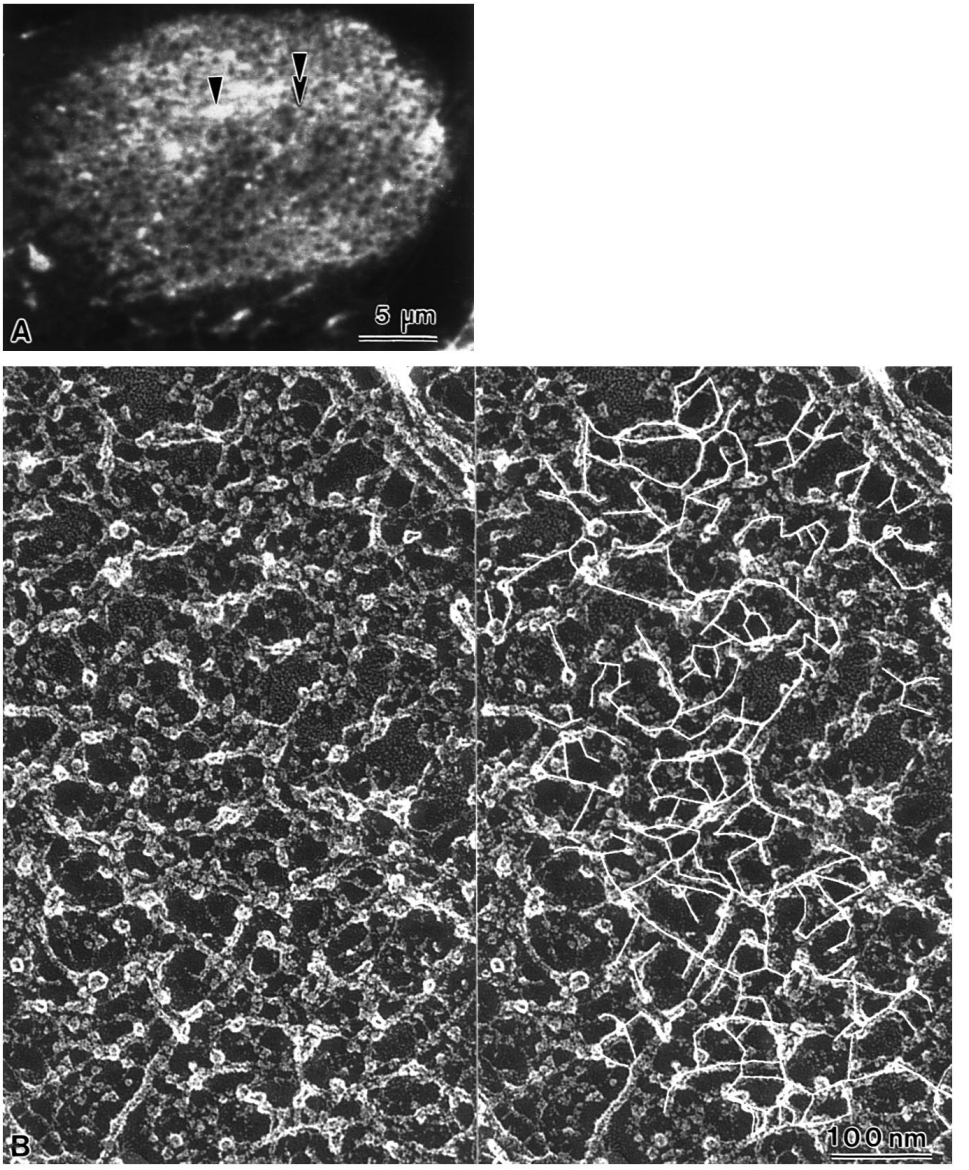

Fig. 2. An extensive area of membrane skeleton used to measure filament lengths and connectivity. To avoid obscuring intersections, this cluster was labeled with fluorescent toxin, but not with antibodies. The replicated skeleton (B) corresponds to a bright area (double arrowhead) in the fluorescence micrograph (A). In other areas that appeared brighter by R-BT fluorescence (single arrowhead in A), the membrane skeleton was overlain with additional cytoskeleton and could not be analyzed. The micrograph of the replica was digitized, filaments were traced with a computer graphics program, and the tracing was superimposed on one micrograph of the stereo pair (B). Filament lengths were then measured from a enlarged print of the tracing, using a graphics tablet. The skeleton includes 111 intersections of 3 filaments, 13 intersections of 4 filaments, and 1 intersection with 5 filaments, for an average connectivity of 3.12.

tified by their correspondence to bright spots of R-BT fluorescence and their distinctive filament network. A group of 14 representative AChR domains contained 114±35 gold particles/μm^2. This labeling was specific, as 35 adjacent clathrin-coated domains contained only 1±3 gold particles/μm^2. Control experiments showed no labeling (<1 gold particle/μm^2) if the primary antibody was omitted or inappropriate secondary antibodies were used. Gold particles were not randomly scattered across AChR domains, but were clearly associated with the filament network. When gaps in the network exposed small areas of the membrane's inner surface, no gold particles decorated the bare membrane.

mAb VIIF7 recognizes an epitope in the beta-1 domain near the carboxy terminus of erythrocyte β-spectrin; this domain lies near the head end of the spectrin dimer in the membrane skeleton of erythrocytes and is important in the formation of spectrin oligomers (Harris et al., 1986). If the corresponding beta-1 domain of the AChR-associated β-spectrin molecule also participates in oligomer formation, then filaments of the AChR domains should be labeled close to their ends by mAb VIIF7. In replicas of AChR domains that were not labeled by antibody, the filaments were always straight and their intersections were easily seen. In labeled replicas, however, filament intersections were often partially obscured by gold particles (compare Fig. 5A with Fig. 2). Therefore, in the tracing of Fig. 5B, filaments partially obscured by VIIF7 label were extended in the same direction to obtain locations of intersections. The fact that these 'extrapolated intersections' were obscured by overlying gold particles itself suggests that the antibodies are labeling close to intersections. This idea was tested more rigorously by measuring the lengths of filaments from their unlabeled ends to the edge of the platinum-shadowed gold particle (the 'end-to-label length' indicated in Fig. 5B) and the total lengths of the same filaments from the visible end to the extrapolated intersection (the 'total length' indicated in Fig. 5B). The ratio of lengths was 0.71±0.13 (72 labeled filaments from 2 AChR domains), which is significantly different (P<.0001, t-test) from the ratio of 0.5 that would be expected if filaments were labeled at their midpoints or randomly along their length. Since the measurement is taken

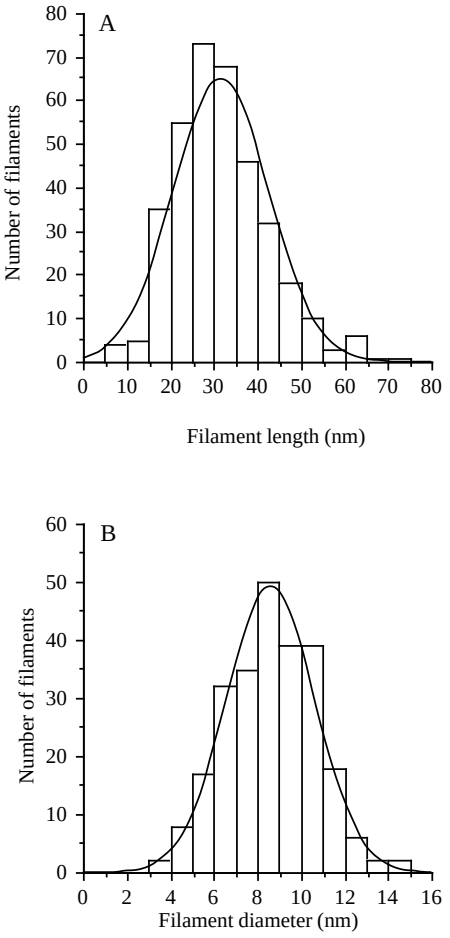

Fig. 3. Lengths and diameters of filaments in the membrane skeleton have normal Gaussian distributions. The histogram of filament lengths (A) was obtained from measurements on 357 filaments in 4 AChR-rich regions of 3 clusters. The solid line shows the Gaussian distribution having the same mean and standard deviation (31.7±10.9 nm). The histogram of filament diameters (B) was obtained from measurements on 250 filaments in the same AChR-rich regions. The solid line shows the Gaussian distribution having the same mean and standard deviation (8.6±2.0 nm).

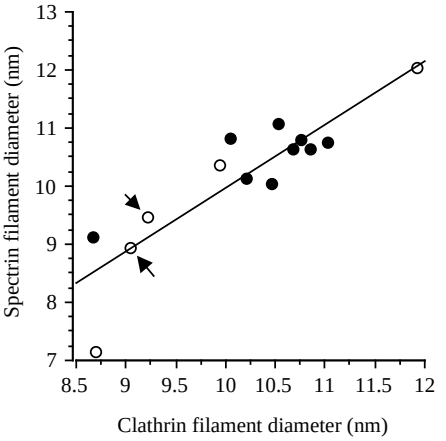

Fig. 4. Filament diameters vary with the amount of platinum deposition. Diameters of 50 filaments in AChR domains and 30-50 filaments in nearby clathrin domains were measured in each of several micrographs, and the average diameters for each micrograph were plotted against each other. The average diameters of the two types of filament were highly correlated ($P<.0001$), suggesting that both are affected by the amount of platinum deposited on them. Filled circles represent data from 4 samples that were replicated simultaneously. Open circles were obtained from replicas used for measurements of filament lengths. Arrows indicate data from 2 areas of the same replica.

Table 1. Characteristic parameters of membrane skeletons of erythrocytes and AChR domains

	Erythrocyte	AChR domain
Filament length (nm)	28.8±8.7*,†	31.7±10.9
Filament diameter (nm)	7.8±2.0*,†	8.6±2.0
simultaneous replication‡	9.1±1.2	10.5±1.8
Filaments/intersection	3.4*	3.1-3.3
Intersections/μ§	411*	500 (unlabeled domain) 180,280 (labeled domains)
Intramembrane particles/μ†	~3,000	733±22§

*Data from Ursitti et al., 1991.

†Data on spectrin filaments published in a previous review (Pumplin and Bloch, 1993) were based on fewer measurements than are presented here. Given the large standard deviation (11 nm, or about 1/3 the filament length), the differences in means are not significant. Filaments in situ are shorter and more variable in length than the extended filaments found in spread erythrocyte skeletons, consistent with the idea that these filaments are formed from flexible molecules that are variably extended. The diameter of spectrin filaments given in the review is smaller because it was corrected for the contribution of the metal shadow.

‡Two samples of erythrocyte ghosts and four myotubes were etched and replicated simultaneously. More platinum was deposited in this experiment than in previous replications, resulting in increased diameters of both erythrocyte and AChR domain filaments. See Materials and Methods and Fig. 4 for details.

§Data from Pumplin and Bloch, 1987.

from the unlabeled end of the filament, the labeling gold particle is less than 30%, or 10 nm, from the end of an average 32 nm long filament. Measuring to the edge of the platinum shadow makes this a conservative estimate; taking the center of the gold particle as the site of labeling would make this site ~5 nm from the labeled end.

In order to understand how spectrin is arranged in the filaments, I analyzed further the pattern of immunogold labeling. Filaments in the network could contain β-spectrin as monomers, parallel homodimers, or antiparallel homodimers; additionally, filaments could be heterodimers with both α and β subunits (Fig. 6). Of these possibilities, only the antiparallel homodimer arrangement gives filaments that are symmetric with regard to an epitope located at one end of β-spectrin, while the other arrangements result in filaments that have the epitope located only at one end. The expected labeling positions are shown in Fig. 6. If filaments are asymmetric and intersections are formed from ends that are antigenically similar, then networks formed from such filaments will contain intersections of two different types. This is the case for erythrocyte skeletons, where 'head' ends of spectrin tetramers are linked together via interactions between the α and β subunits (Speicher et al., 1993) while 'tail' ends of tetramers bind actin (Cohen et al., 1980). On the other hand, if symmetric filaments are assembled into a network, the resulting intersections are all antigenically similar (Fig. 6).

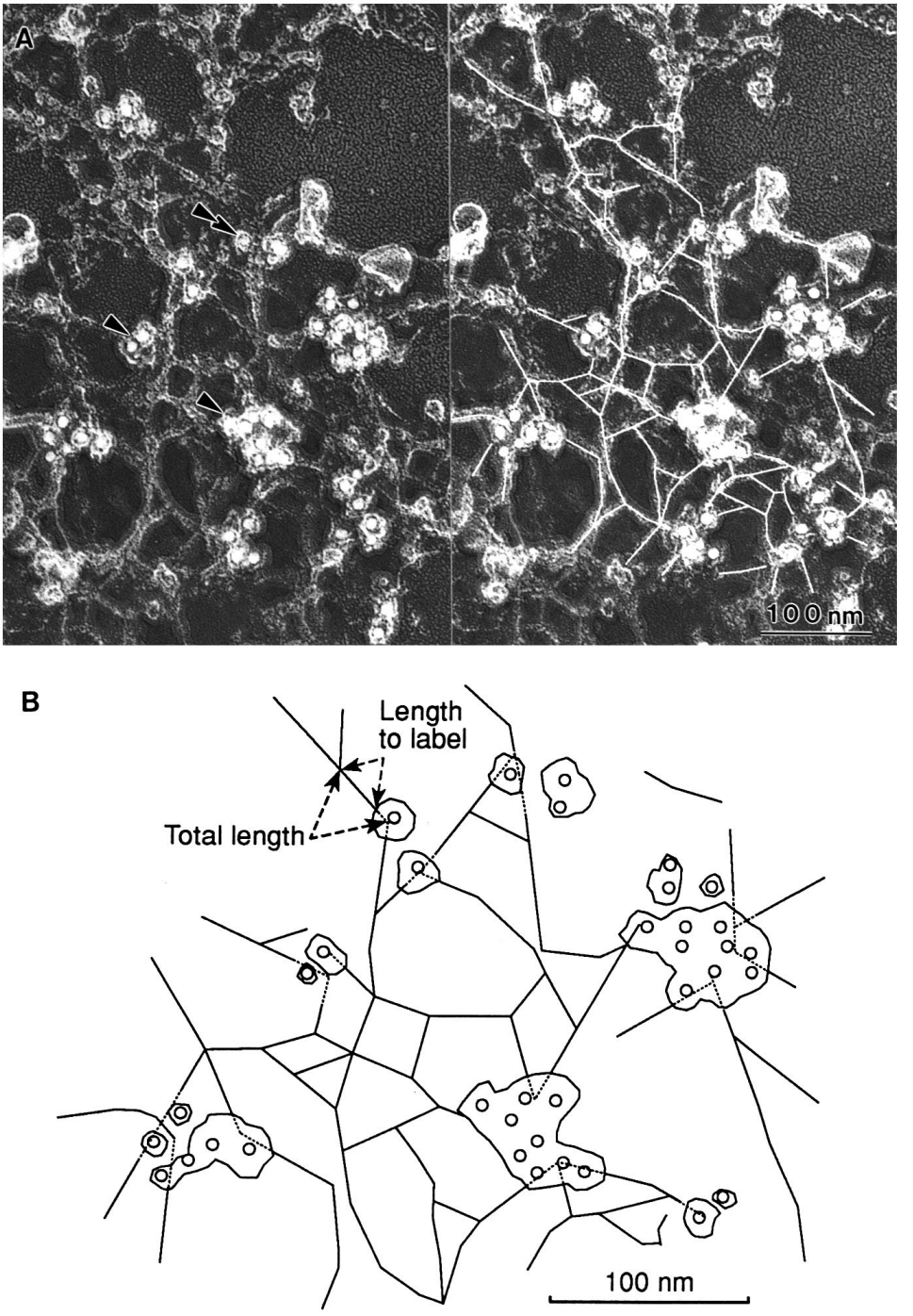

Fig. 5. (A) The membrane skeleton consists of a network of intersecting filaments containing spectrin. After shearing, the cluster was labeled with a monoclonal anti-β-spectrin antibody (VIIF7) followed by a rabbit anti-mouse IgG and goat anti-rabbit IgG adsorbed to 10 nm colloidal gold particles. Gold particles (arrowheads) decorate the filament network, but do not appear in areas lacking the network. To illustrate the network more clearly, the micrograph was digitized, filaments were traced with a computer graphics program, and the tracing was superimposed on one micrograph of the stereo pair. Gold particles preferentially decorate filaments near their ends, obscuring the intersections; several examples involving single gold particles are indicated (double arrowhead). This micrograph lies in the region boxed in Fig. 1B and C. (B) Gold particles marking binding sites of mAb VIIF7 lie preferentially at the ends of filaments in AChR domains. A portion of the filament tracing in A is shown at higher magnification. Tracings of filaments (solid lines) are projected (dotted lines) to intersection points lying beneath collections of gold particles (solid lines surrounding 10 nm circles at positions of gold particles). Arrows indicate segments of a filament from one end to the edge of the platinum shadow (end-to-label) and the total length of a filament between one visible and one obscured end (total length). Similar measurements were used to show that gold particles were concentrated at the ends of filaments in a non-random fashion. See text for details.

The antigenic similarity of intersections was tested with the antibody VIIF7 that binds close to intersections in the membrane skeletal network. The antibody was used under less than saturating conditions to avoid obscuring intersections with gold particles. Portions of AChR domains from 3 different replicas were analyzed, in which 18-20% of the intersections were labeled with gold particles (Fig. 7). I paired each labeled intersection with its nearest labeled neighbor and measured the distance between the intersections in terms of the number of filaments separating them. Reciprocal pairs were counted only once. In 65-80% of the pairs, the labeled intersections were adjacent to each other, separated by only 1 filament. In another 15-30% of the pairs, the labeled intersections were separated by two filaments, while pairs of labeled intersections separated by 3 or more filaments were rare (data points in Fig. 8). I then determined whether this pattern could be generated by random labeling of the intersections, given the overall percentage of labeling actually observed. Filaments in the actual networks formed irregular groups of linked polygons, primarily of 3-5 sides. (Two networks with a total of 133 polygons contained 23% triangles, 36% quadrilaterals, 19% pentagons, and 22% polygons with 6 or more sides). I simulated these networks with groups of 150 consecutively-numbered intersections in 10 columns and 15 rows whose intervening edges formed quadri-

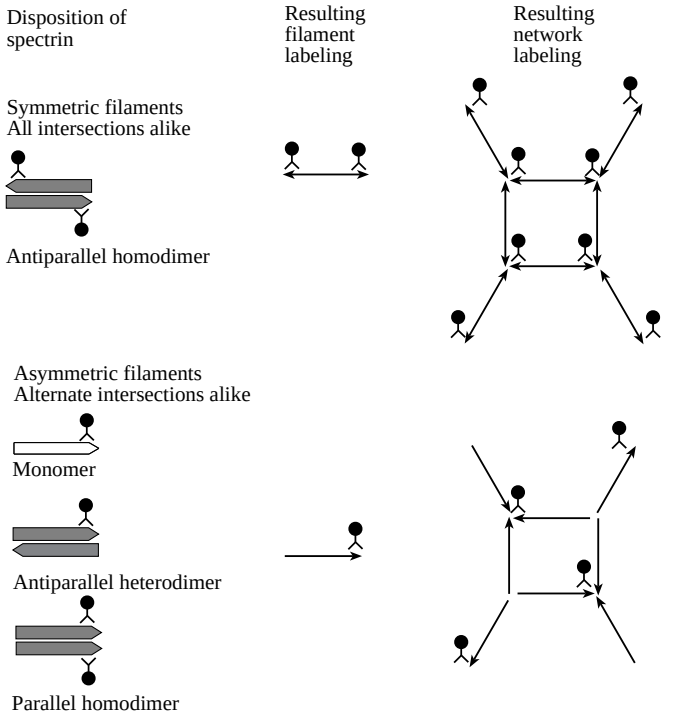

Fig. 6. Possible arrangements of spectrin molecules within a membrane skeleton. Spectrin molecules are depicted diagrammatically (β-spectrin shown in white; α-spectrin shown stippled) with points indicating the 'head' ends, the region of VIIF7 binding to β-spectrin. Spectrin molecules disposed as antiparallel homodimers (upper left) generate symmetric filaments that can be labeled at both ends. These symmetric filaments assemble into networks all of whose intersections can be labeled (upper right). Spectrin molecules in other arrangements (lower left) generate asymmetric filaments whose ends differ immunologically; a particular monoclonal antibody binds only to one end. These asymmetric filaments assemble into networks whose intersections contain only heads or tails, and are therefore immunologically distinguishable from their nearest neighbors (lower right); a particular mAb binds to alternate intersections.

laterals and triangles, respectively. For each of these theoretical networks, a computer program 'labeled' 20% of the intersections; intersections to be labeled were chosen at random. The program then determined the distances between nearest-neighbor pairs of labeled intersections in terms of the number of edges forming the shortest path connecting the intersections. This process was repeated 1,000 times for each type of network and the results were expressed as a histogram of the fraction of nearest-neighbor pairs separated by a given number of sides (Fig. 8, solid and dot-dash lines). The fit of actual data points to the histograms shows that the pattern of labeling in actual networks can be generated assuming random labeling of all the intersections in a network of triangles or quadrilaterals. The histograms generated with networks of triangles and quadrilaterals, as well as hexagons (data not shown), were not very different from each other, and the labeling properties of the actual network should be similar as it contains all these types of polygons.

Alternatively, in a network of quadrilaterals formed by asymmetric filaments and having intersections composed solely of either heads or tails of these filaments, intersections of filament 'heads' would be adjacent only to intersections of filament 'tails' and vice versa (Fig. 6). Simulated labeling of a network of quadrilaterals with intersections alternating in this way generated a histogram with no nearest neighbors separated by 1 edge and 91% of nearest neighbors separated by 2 filaments (Fig. 8, dotted line); this is quite different from the actual data. Simulations on networks of triangles and hexagons with alternating intersections gave essentially identical results.

Thus, the distribution of labeling I observed is consistent with all intersections being susceptible to labeling with mAb VIIF7. In turn, this implies that the membrane skeleton of AChR domains is made up of immunologically symmetric filaments. β-spectrin in these filaments must be present as antiparallel homodimers.

One complication of this analysis of intersection labeling arises from the fact that individual intersections may differ in their ability to bind antibody. Since a given intersection could be labeled by binding the mAb to any one of the filaments present at that intersection, multiple labeling of intersections is

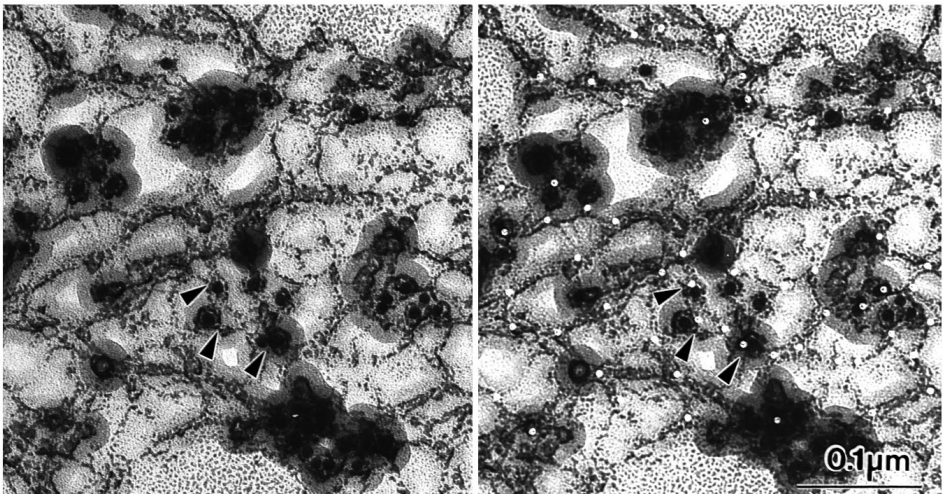

Fig. 7. Labeling of intersections by gold particles marking binding sites of mAb VIIF7. The membrane skeleton at an AChR domain is shown in reverse contrast for clarity (platinum and gold particles dark, shadows white). White dots generated with a computer graphics program indicate positions of intersections, while larger dark dots are gold particles surrounded by 'halos' of platinum and carbon. Dotting the intersections facilitated determining the spacing between pairs of labeled intersections. Arrowheads indicate 3 labeled intersections connected by 1 (upper pair) or 2 (lower pair) filaments, respectively. This and similar pictures were used to determine the number of pairs of labeled intersections connected by paths containing 1,2,3,4, and >4 filaments as well as the number of labeled intersections. These were then expressed as fractions of the total number of intersections in the micrograph.

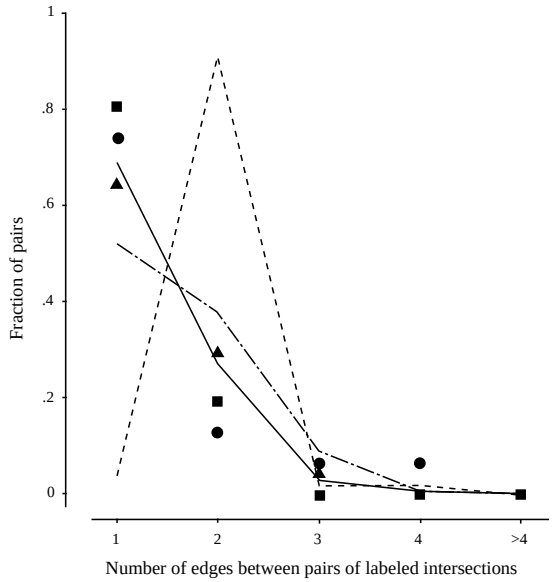

Fig. 8. The distribution of immunogold labeling is consistent with all intersections being capable of binding mAb VIIF7. The number of nearest-neighbor pairs of labeled intersections connected by paths containing 1,2,3,4, and >4 filaments were determined for three AChR domains as shown in Fig. 7, and expressed as fractions of the total number of labeled pairs. These domains had 31 (squares), 31 (circles), and 20 (triangles) pairs of labeled intersections, respectively, and came from independent replicas. The fractions of pairs separated by different numbers of edges were compared with theoretical distributions based on random labeling of 20% of all intersections under one of the following models: (1) All intersections in a network of triangles could be labeled (solid line); (2) All intersections in a network of quadrilaterals could be labeled (dot-dash line); (3) Alternating intersections in a network of quadrilaterals could be labeled (broken line). The actual data were approximated more closely by models predicting that all intersections were equally likely to be labeled (solid and dot-dash lines) than under the model assuming that only alternate intersections could be labeled (broken line). See text for details.

possible. I simulated this by running the labeling algorithm for intersections 3 times (assuming an average of 3 edges/intersection) using a frequency of labeling sufficient to guarantee that about 20% of intersections would be labeled at least once. Some intersections were labeled two or three times by this procedure, but the resulting histogram of nearest-neighbor pairs was nearly identical to that obtained when only singly labeled intersections were allowed.

A second complication arises if intersections can contain both ends of asymmetric filaments. If 'head' ends of asymmetric filaments could bind to 'tail' ends, then intersections could contain both 'heads' and 'tails' in all possible combinations (3H, 2H:1T,1H:2T, 3T). Assuming that all combinations are equally probable, these intersections would be present in the ratio of 1:3:3:1. This possibility amounts to having some intersections that are more likely to be labeled than others (since they contain more antibody binding sites near the head end), but the overall distribution of intersections that are labeled at least once would be the same as that obtained under the assumption that all intersections are equally susceptible to labeling at a given overall frequency. Thus, the analysis of labeling cannot distinguish between asymmetric filaments with mixed intersections containing both heads and tails and symmetric filaments with only one type of intersection. Although head-to-tail binding of spectrin subunits in AChR domains cannot be ruled out, it apparently does not occur in erythrocytes, and thus is a less likely possibility than is symmetric filaments generated by antiparallel homodimers.

DISCUSSION

The results presented here confirm that an unusual isoform of β-spectrin is closely associated with clustered AChR and is present in a network resembling that found in quick-freeze, deep-etch views of the postjunctional cytoplasm. Although the network at AChR domains has not yet been isolated in sufficient purity and quantity for biochemical analysis, the organization of spectrin within this network can be inferred from the filament dimensions and the pattern of antibody labeling. With the possible exception of a requirement for actin oligomers (see below), the data are consistent with a network composed of antiparallel homodimers of β-spectrin, as postulated earlier (Bloch and Morrow, 1989).

Despite its unusual composition and homodimeric organization, the network at AChR domains is remarkably similar to the spectrin-based membrane skeleton of human erythrocytes. In erythrocytes and other tissues, spectrin consists of both alpha and beta subunits linked into antiparallel heterodimers. The filaments seen by QFDERR of erythrocytes have the size expected for a spectrin dimer (Ursitti et al., 1991). The filaments at AChR domains are also likely to be dimers, since they are very similar in size to those of erythrocytes. Two lines of evidence suggest that these are antiparallel homodimers of β-spectrin. First, no alpha subunit was identified at AChR domains (Bloch and Morrow, 1989), although this may indicate an unusual isoform that is not recognized by the available antibodies. Second, if β-spectrin forms filaments composed of antiparallel homodimers, then mAb VIIF7 should bind equally well to all the filament intersections, and this is consistent with the decoration pattern obtained with immunogold labeling. Formation of parallel dimers has not been reported for proteins of the spectrin family, and would also create networks with intersections that are not immunologically equivalent.

mAb VIIF7 binds close to the ends of filaments, consistent with the binding of this mAb to a region analogous to one that is active in the head-to-head oligomerization of erythrocyte spectrin. Linking antiparallel homodimers of β-spectrin together head-to-head could generate an extended network without the need for the actin oligomers present in erythrocytes. However, each end of an antiparallel homodimer would contain one copy of the N-terminal region of β-spectrin. The homologous region of erythrocyte β-spectrin binds actin. If this region of AChR-domain β-spectrin has a similar actin-binding site, then either end of a filament could theoretically bind to an actin oligomer. An isoform of actin does occur in AChR domains and is removed by some of the same conditions that extract spectrin (Bloch, 1986), suggesting that it is a component of the network. Actin-binding 'tails' of spectrin filaments in erythrocyte ghosts were decorated by a specific mAb (VD4; Ursitti et al., 1991); unfortunately, this antibody

does not label AChR domains (Bloch and Morrow, 1989) and I have been unable to immunogold label AChR domains with anti-actin antibodies. Thus it is not clear whether some of the actin at AChR domains forms short oligomers like those of the erythrocyte skeleton, nor whether these are present at filament intersections.

The network at AChR domains of myotubes is essentially identical in filament lengths and connectivity to the 'gold standard' of spectrin-based membrane skeletons, that of the erythrocyte. The variability in lengths of spectrin filaments was noted previously in cytoskeletons of erythrocyte ghosts viewed by QFDERR (Ursitti et al., 1991), and is likely to be due to variations in folding between the successive 106 amino-acid repeat units that make up the spectrin molecule (Bloch and Pumplin, 1992). When fixed in situ, the extensible spectrin molecules of erythrocytes remain straight even though they are only about one third of their fully extended length; spectrin filaments in AChR domains are likely to behave similarly. The average diameter of filaments in AChR domains was slightly larger than that of filaments in erythrocytes (Ursitti et al., 1991). Simultaneous replication of AChR clusters and erythrocyte ghosts showed that this difference was independent of the amount of platinum applied during replication. It may reflect contributions from minor components to some filaments in the AChR-domain skeleton. Dystrophin is likely to contribute to some filaments in the membrane skeleton, since the molecule is long and flexible and anti-dystrophin antibodies label the network at AChR domains; it probably cannot account for many of them, however, given its apparently low incidence (~4%) compared to spectrin (Dmytrenko et al., 1993). Dystrophin-related protein (utrophin) has a similar structure to that of dystrophin (Tinsley et al., 1992) and is present at AChR clusters of cultured C2 myotubes (Phillips et al., 1993). Semiquantitative fluorescence measurements suggest that utrophin is about twice as abundant as dystrophin in AChR clusters (R. Bloch, D. Pumplin et al., unpublished), but these measurements suggest that the two proteins together could only account for ~15% of the filaments at AChR domains. Details of the relation between dystrophin, utrophin and spectrin filaments require further immunogold labeling and analysis, but the labeling seen thus far (Dmytrenko et al., 1993) did not rule out the possibility that dystrophin and spectrin are present in the same filament. Unfortunately, it was not possible to determine directly whether all filaments could be labeled using a higher concentration of primary antibody because VIIF7 as well as a polyclonal anti-spectrin antibody previously used to label myotubes (Bloch and Morrow, 1989) are no longer available.

Some other quantitative aspects are worth noting. The portions of AChR domains analyzed contained 180-500 intersections/μm^2, similar to the density found in the erythrocyte (Table 1). The lower values found for labeled areas reflect a choice of networks that had relatively lower densities of filaments and were therefore easier to analyze. Since each intersection has an average of 3.2 'head' ends with VIIF7 binding sites, there are $5\text{-}16\times10^2$ binding sites/μm^2. This is comparable to the density in AChR domains of both IMP ($7\times 10^2/\mu m^2$; Table 1) and AChR ($10\text{-}20\times10^2/\mu m^2$; see references in Bloch and Pumplin, 1987), and would allow all AChR molecules to be immobilized by binding to spectrin. Such binding is consistent with the preferential association of IMP with filaments demonstrated by combined QFDERR and freeze fracture (Pumplin, 1992; D. W. Pumplin, unpublished). However, this similarity between the number of AChR and spectrin molecules is inconsistent with semiquantitative fluorescence measurements indicating 4-7 spectrin molecules per AChR in clusters fixed within a few seconds of shearing. Some of this spectrin may be more loosely bound to the membrane, however, as it is shed during the isolation of clusters by saponin extraction (Bloch and Morrow, 1989). Moreover, clusters used for QFDERR were deliberately chosen to have minimal amounts of cytoskeleton remaining after shearing, and these clusters may well retain only the spectrin that is most tightly bound.

It is now clear that spectrin-based membrane skeletons are present in many cells and that these skeletons share common functions, acting to support the membrane and anchor intramembrane proteins. Similarities between the organization of spectrin in relatively accessible skeletons such as those of erythrocytes, platelets, and AChR-rich domains (Pumplin and Bloch, 1993) suggest that studies on these domains will continue to yield the information needed to understand how spectrin, together with its anchoring and intramembrane proteins, are organized in other cells.

I thank W. Resneck and A. O'Neill for preparation of cultures, J. Morrow for the gift of mAb VIIF7, R. Bloch for hours of discussion, J. Strong for expert assistance with QFDERR and EM, and the reviewers for several helpful suggestions. This work was supported by grants from NIH (NS 15513) and the Muscular Dystrophy Association.

REFERENCES

Aggeler, J. and Werb, Z. (1982). Initial events during phagocytosis by macrophages viewed by quick-freeze, deep-etch. *J. Cell Biol.* **94**, 613-623.

Avnur, Z. and Geiger, B. (1981). Substrate-attached membranes of cultured cells. Isolation and characterization of ventral cell membranes and the associated cytoskeleton. *J. Mol. Biol.* **53**, 361-379.

Axelrod, D., Ravdin, P. M. and Podleski, T. R. (1978). Control of acetylcholine receptor mobility and distribution in cultured muscle membranes. A fluorescence study. *Biochim. Biophys. Acta* **511**, 23-38.

Bennett, V. (1990). Spectrin-based membrane skeleton: a multipotential adaptor between plasma membrane and cytoplasm. *Physiol. Rev.* **70**, 1029-1065.

Birks, R., Huxley, H. E. and Katz, B. (1960). The fine structure of the neuromuscular junction of the frog. *J. Physiol.* **150**, 134-144.

Bloch, R. J. (1979). Dispersal and reformation of acetylcholine receptor clusters of cultured rat myotubes treated with inhibitors of energy metabolism. *J. Cell Biol.* **82**, 626-43.

Bloch, R. J. and Geiger, B. (1980). The localization of acetylcholine receptor clusters in areas of cell-substrate contact in cultures of rat myotubes. *Cell* **21**, 25-35.

Bloch, R. J. (1986). Actin at receptor-rich domains of isolated acetylcholine receptor clusters. *J. Cell Biol.* **102**, 1447-1458.

Bloch, R. J. and Froehner, S. C. (1987). The relationship of the postsynaptic 43kd protein to acetylcholine receptors in receptor clusters isolated from cultured rat myotubes. *J. Cell Biol.* **104**, 645-654.

Bloch, R. J. and Pumplin, D. W. (1988). Molecular events in synaptogenesis: nerve-muscle adhesion and postsynaptic differentiation. *Am. J. Physiol.* **254**, C345-C364.

Bloch, R. J. and Morrow, J. S. (1989). A unique beta-spectrin associated with clustered acetylcholine receptors. *J. Cell Biol.* **108**, 481-493.

Bloch, R. J., Resneck, W. G., O'Neill, A., Strong, J. and Pumplin, D. W. (1991). Cytoplasmic components of acetylcholine receptor clusters of cultured rat myotubes: the 58-kD protein. *J. Cell Biol.* **115**, 435-446.

Bloch, R. J. and Pumplin, D. W. (1992). A model of spectrin as a concertina in the erythrocyte membrane skeleton. *Trends Cell Biol.* **2**, 186-189.

Cohen, C. M., Tyler, J. M. and Branton, D. (1980). Spectrin-actin associations studied by electron microscopy of shadowed preparations. *Cell* **21**, 875-883.

Daniels, M. P. (1990). Localization of actin, beta-spectrin, 43×10^3 M_r and 58×10^3 M_r proteins to receptor-enriched domains of newly formed acetylcholine receptor aggregates in isolated myotube membranes. *J. Cell Sci.* **97**, 615-626.

Dmytrenko, G. M., Pumplin, D. W. and Bloch, R. J. (1993). Dystrophin at AChR clusters of cultured rat myotubes. *J. Neurosci.* **13**, 547-558.

Froehner, S. C. (1993). Regulation of ion channel distribution at synapses. *Annu. Rev. Neurosci.* **16**, 347-368.

Harris, A. S., Anderson, J. P., Yurchenco, P. D., Green, L. A., Ainger, K. J. and Morrow, J. S. (1986). Mechanisms of cytoskeletal regulation: functional and antigenic diversity in human erythrocyte and brain beta spectrin. *J. Cell Biochem.* **30**, 51-69.

Hirokawa, N. and Heuser, J. E. (1982). Internal and external differentiations of the postsynaptic membrane at the neuromuscular junction. *J. Neurocytol.* **11**, 487-510.

Luther, P. W. and Bloch, R. J. (1989). Formaldehyde-amine fixatives for immunocytochemistry of cultured Xenopus myocytes. *J. Histochem. Cytochem.* **37**, 75-82.

Marchesi, V. T. (1985). Stabilizing infrastructure of cell membranes. *Annu. Rev. Cell Biol.* **1**, 531-561.

Phillips, W. D., Noakes, P. G., Roberds, S. L., Campbell, K. P. and Merlie, J. P. (1993). Clustering and immobilization of acetylcholine receptors by the 43-kD protein: a possible role for dystrophin-related protein. *J. Cell Biol.* **123**, 729-740.

Pumplin, D. W. and Bloch, R. J. (1987). Disruption and reformation of the acetylcholine receptor clusters of cultured rat myotubes occur in two distinct stages. *J. Cell Biol.* **104**, 97-108.

Pumplin, D. W. (1989). Acetylcholine receptor clusters of rat myotubes have at least three domains with distinctive cytoskeletal and membranous components. *J. Cell Biol.* **109**, 739-753.

Pumplin, D. W., Luther, P. W., Samuelsson, S. J., Ursitti, J. A. and Strong, J. (1990). Quick-freeze, deep-etch replication of cells in monolayers. *J. Electron. Microsc. Tech.* **14**, 342-347.

Pumplin, D. W. (1992). Simultaneous views of the cytoskeleton and intramembrane particles at membrane domains rich in acetylcholine receptors or clathrin. *Mol. Biol. Cell* **3**, 365a.

Pumplin, D. W. and Bloch, R. J. (1993). The membrane skeleton. *Trends Cell Biol.* **3**, 113-117.

Ravdin, P. and Axelrod, D. (1977). Fluorescent tetramethylrhodamine derivatives of alpha-bungarotoxin: preparation, separation, and characterization. *Anal. Biochem.* **80**, 585-92.

Speicher, D. W., DeSilva, T. M., Speicher, K. D., Ursitti, J. A., Hembach, P., and Weglarz, L. (1993). Location of the human red cell spectrin tetramer binding site and detection of a related 'closed' hairpin loop dimer using proteolytic footprinting. *J. Biol. Chem.* **268**, 4227-4235.

Stya, M. and Axelrod, D. (1983). Mobility and detergent extractability of acetylcholine receptors on cultured rat myotubes: a correlation. *J. Cell Biol.* **97**, 48-51.

Tatsuoka, H., Kadota, T. and Kono, K. (1988). Postsynaptic arch in the frog neuromuscular junction; paramembranous protuberances coating the inner surface of the postjunctional membrane. *J. Neurocytol.* **17**, 87-94.

Tinsley, J. M., Blake, D. J., Roche, A., Fairbrother, U., Riss, J., Byth, B. C., Knight, A. E., Jones, J., Suthers, G. K., Love, D. R. et al. (1992). Primary structure of dystrophin-related protein. *Nature* **360**, 591-3.

Ursitti, J. A., Pumplin, D. W., Wade, J. B. and Bloch, R. J. (1991). Ultrastructure of the human erythrocyte cytoskeleton and its attachment to the membrane. *Cell Motil. Cytoskel.* **19**, 227-243.

(Received 3 January 1995 - Accepted 20 June 1995)